International Journal of Civil Engineering and Technology (IJCIET)
Volume 8, Issue 3, March 2017, pp. 302–313 Article ID: IJCIET_08_03_031
Available online at http://www.iaeme.com/IJCIET/issues.asp?JType=IJCIET&VType=8&IType=3
ISSN Print: 0976-6308 and ISSN Online: 0976-6316

STRUCTURAL ANALYSIS ON WING BOX SPLICED JOINT FOR AN AIRCRAFT USING FINITE ELEMENT METHOD

T. Narendiranath Babu
School of Mechanical Engineering, VIT University, Vellore, India

Prasanth
School of Mechanical Engineering, VIT University, Vellore, India

E. Raj Kumar
School of Mechanical Engineering, VIT University, Vellore, India

R. Mageshvaran
School of Electrical Engineering, VIT University, Vellore, India

T. Shankar
School of Electronics Engineering, VIT University, Vellore, India

D. Rama Prabha
School of Electrical Engineering, VIT University, Vellore, India

ABSTRACT

The attachment joints are inevitable in any large structure like an airframe. Splicing is normally used to retain a clean aerodynamic surface of the wing skin. The wings are the most important lift-producing part of the aircraft. Wings vary in design depending upon the aircraft type and its purpose. The wing box has two crucial joints, the skin splice joint and spar splice joint. Top and bottom skins of inboard and outboard portions are joined together by means of skin splicing. Front and rear spars of inboard and outboard are joined together by means of spar splicing. The skins resist much of the bending moment in the wing and the spars resist the shear force. In this study the chord-wise splicing of wing skin is considered for a detailed analysis. The splicing is considered as a multi row riveted joint under the action of tensile in plane load due to wing bending. The stress analysis of the joint was carried out to predict the stresses at rivet holes due to by-pass load and bearing load. The stresses were calculated using the finite element method with the aid of PATRAN/NASTRAN. A fatigue crack will appear at the location of high tensile stress in an airframe structure. Further these locations are invariably the sites of high stress concentration were studied. The life prediction of structural members are requires a model for fatigue damage build up. The stress life curve data for various stress ratios and local

stress analysis was calculated to find the stress concentration. The response plots of the splice joint aircraft structure were estimated. The splice joint is one of the critical locations where fatigue crack starts to initiate. In this work estimation of fatigue life for crack initiation of splice joint structure were carried out at maximum stress location.

Key words: Finite element approach, stress analysis, splices joint structure, wing box analysis, top skin analysis, bottom skin analysis.

Cite this Article: T. Narendiranath Babu, Prasanth, E. Raj Kumar, R. Mageshvaran, T. Shankar and D. Rama Prabha, Structural Analysis on Wing Box Spliced Joint for an Aircraft Using Finite Element Method. *International Journal of Civil Engineering and Technology*, 8(3), 2017, pp. 302–313.
http://www.iaeme.com/IJCIET/issues.asp?JType=IJCIET&VType=8&IType=3

1. INTRODUCTION

Now a days the stress analysis and fatigue life[1] prediction for splice joint in an aircraft fuselage using finite element method. An aluminium alloy 2024-T351 material was used for aircraft structural elements of the panel for production of the aircraft body. For the fuselage structure, the force due to cabin pressurization is considered as one of the critical load cases Fuselage structure has the capabilities of constant amplitude load cycles due to pressurization. Splice joints are used for the fuselage structure in aircrafts. The typical splice joint panel containing of skin plates, double plate and stiffener were considered for further studies. This paper presents the stress analysis of a splice joint in a transport aircraft. A two-dimensional finite element-analysis was carried out in the splice joint aircraft panel. Further, the distribution of fasteners loads and local stress field at rivet locations were studied using finite element analysis approach. This paper includes the analysis of the splice joint using software's MSC/NASTRAN and MSC/PATRAN. A two-dimensional finite element-analysis was carried out on the splice joint panel aircraft structure. The distribution of fasteners loads and local stress field analysis at rivet locations was carried out through finite element analysis. The work also includes that the modifications required correcting the boundary effects of the panel structure. The global finite element analysis of a segment of typical fuselage was carried out in this structure. This global finite element analysis results will be point of reference for comparing the results from the splice joint panel analysis. The FEA iterations were carried out to get the response of the fuselage structure at the joint location. The splice joint is one of the important locations for fatigue crack to initiation. Therefore, the response of the splice joint is assessed. Hence, the estimate of fatigue life for crack initiation is carried out at maximum stress location.

The main objective of the research was to establish a link between critical riveting process parameters on the potential of fatigue damage[2] in the joint. Aircraft fuselage splices are fatigue critical structures and the damage associated with these structures has been widely recognized as a safety issue that needs to be addressed in the structural integrity of aging aircraft. An effective means for structural evaluations of airworthiness of aging aircraft and obtaining essential data for evaluation of such type of fatigue cracking is airframe teardown inspections and laboratory fatigue testing of lap joint. The Federal Aviation Administration and Delta Airlines teamed up in such an effort to conduct destructive evaluation, inspection and extended fatigue testing of a retired Boeing 727-232 (B727) passenger aircraft near its design service goal Preliminary visual inspection revealed a large number of cracks in the aircraft fuselage lap joint emanating from the rivet/skin interface. Most of these cracks were observed in the lower skin such that they could not be detected under an operator's routine

maintenance. The presence of these cracks was attributed to the sharp gradients of stress arising from contact between the installed rivet and rivet holes.

The failure analysis of various aircraft components[3] due to fatigue and gave recommendations for the problems. After performing the failure analysis of the tail gearbox of the helicopter they concluded that due to location of sharp corners on the boss of tail gear multiple crack generated and they recommended to avoid sharp corners on the boss. Analysing the failure of stainless steel bolts due to corrosion[4] and residual stress in catia .Failure happened due to conjoint action of a surface tensile[5] stress and corrosive environment. Finally they concluded that material of the clamp bolt should be changed into a more corrosion resistance material rather than frequently inspection. To improve the service life[6] of aircraft bottom skin and stringer joint by introducing one more flange near the bottom flange of I-section. We can't stop the crack growth rate but by introducing one more flange at least we can increase the service life of structure.

The work carried out on fatigue failure and cracking[7] of aircraft wheel rim. The wheel was made from 2014-T6 aluminum alloy. Inspection of air craft components are carried out by various methods. One of the method is non-destructive testing. They observed that during the manufacturing of tire a strong textile net is incorporated. In worn-out tires the net is in direct contact with the rim surface. Due to this high stresses developed and fatigue crack developed. The wing-fuselage connector corrosion, crack initiation[8] and fatigue life analysis on upper fuselage lugs and lower wing lug using Nastran patron.

The failure of wing bottom skin and stringer spliced joint[9] due to fatigue load and observed crack rate growth due to plastic deformation through fract graphic analysis was done. The fatigue analysis for CF-18 component .was developed for 3-dimensional finite element analysis model to simulate the loading applied in the lug test and determined the local stress-strain distribution. Based on the failure mechanisms, a simplified crack model was developed to estimate the crack growth and path of that crack. A linear relation[11] developed between the log of the crack length or depth and the service history by observing the fatigue crack growth and service loads and they observed how cracks have grown from semi and quarter-elliptical surface cuts, holes, pits and inherent material discontinuities.

Modified z-section stringers[12] which are used at top skin to withstand buckling for J-type stingers and also carried out to find out damage tolerance design for bottom skin for crack growth. Analytical methods[13] have been developed based on the complex variational approach for lap joints with single or multiple rivet holes. The joined plates can be either metallic or composite materials. The stresses in the two joined plates and the rivet loads are determined. Finite element analyses are conducted using the commercial packages MSC/Patran and MSC/Nastran. The complete description of an aircraft wing, components of a wing and static loads acting on the wing as shown inFig.1, Fig.2 and Fig.3.

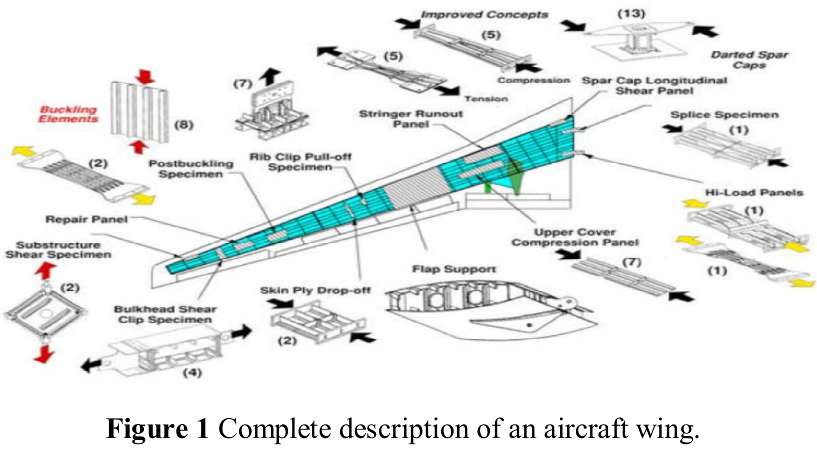

Figure 1 Complete description of an aircraft wing.

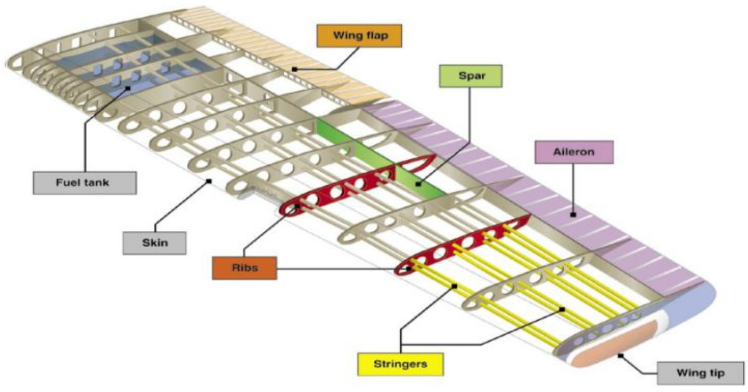

Figure 2 Components of a wing.

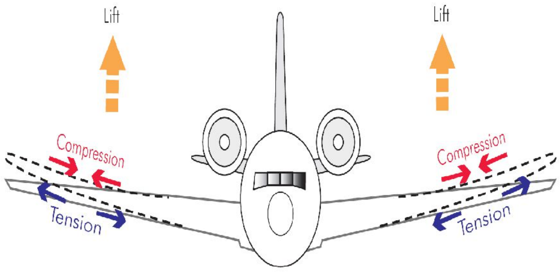

Figure 3 Static Loads acting on wing

2. METHODOLOGY

In this study the chord-wise splicing of wing skin is considered for a detailed analysis. The splicing is considered as a multi row riveted joint under the action of tensile in plane load due to wing bending. Stress analysis of the joint is carried out to compute the stresses at rivet holes due to by-pass load and bearing load. The main objective of this study is global and local stress analysis of the splice joint in an aircraft wing box to compute the stresses at rivet holes due to tension with the help of MSC PATRAN and MSC NASTRAN. The flow chart is shown in Fig.4

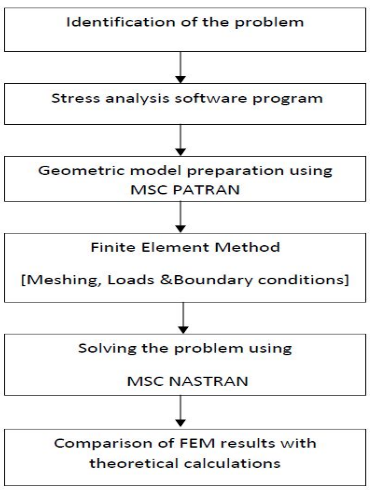

Figure 4 Flow Chart

3. GEOMETRICAL CONFIGARATION

The wing box is modeled in CATIA shown in Fig.5. It consists of different structures. The wing box consists of five ribs including a middle rib, stiffeners, bottom and top skins, spars. Each part is modeled in CATIA software. The assembled wing box with finite element properties is shown in Fig.6.

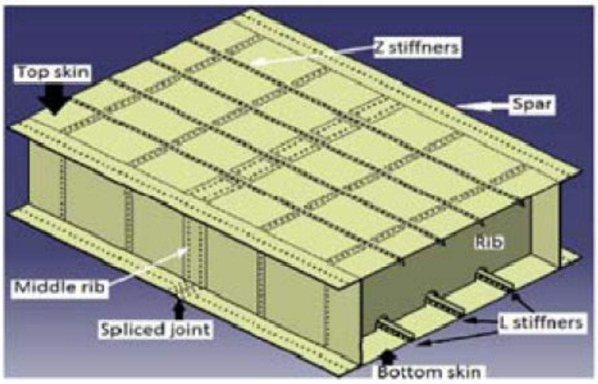

Figure 5 Geometric model of wing box

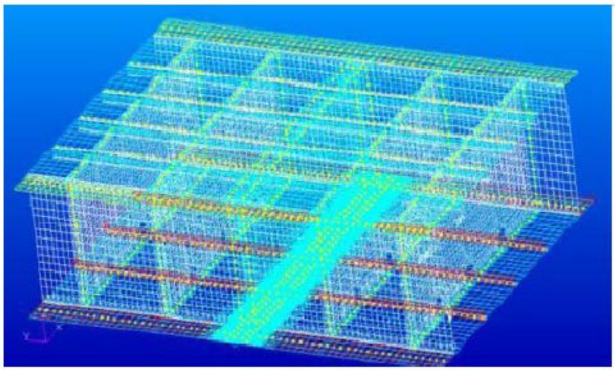

Figure 6 Assembled wing box with finite element properties

3.1. Chemical Composition

The Al 2024-T351 is used in current wing box due to high strength and fatigue resistance properties. The chemical composition of Aluminium (Al) alloy and the physical properties of Al alloy are shown in Table.1 and Table.2.

Table 1 Chemical composition of Al alloy

COMPONENT	Wt. %
Al	90.7-94.7
Cr	Max 0.1
Cu	3.8-4.9
Fe	Max 0.5
Mg	1.2-1.8
Mn	0.3-0.9
Other, each	Max 0.05
Other, total	Max 0.15
Si	Max 0.5
Ti	Max 0.15

Table 2 Physical properties of Al alloy

Young's Modulus	7000 kg/mm^2
Poisson's Ratio	0.3
Density	2800 kg/mm^3
Yield strength	28 kg/mm^2
Ultimate strength	47kg/mm^2

4. LOADS ON THE WING BOX

Lift load is considered as important criteria while designing an aircraft. Fuselage and wings are the two main regions where lift load acting in an aircraft. Here 80% of the lift load is acted on the wings (i.e., maximum lift load is acted on the wings) and remaining 20% in acted on the fuselage. Therefore in wings the maximum load is acted nearer to the wing roots and minimum load is acted at the tip of a wing box.

4.1. Load Calculation for Wing box

Aircraft Category: Medium size (8-10) seater transport aircraft

(a) The all-up weight of the of the aircraft = 2000kg

(b) Design load factor considered = 3g

(c) The total load applied on the aircraft = 6000 kg

(d) Factor of safety (Assumed) = 1.5

(e) Therefore Ultimate load = 9000 kg

(f) The Lift load experienced by both fuselage and wing.

(g) Therefore, Lift load on the wing for 80% = 7200Kg

(h) Load acting on each wing for 20% = 3600kg

(i) Bending moment at the section A-A due to force 3600=3600 x 500=18 x 105 kg-mm

(j) Load at section B - B to produce equivalent Bending Moment at A-A =2400kg

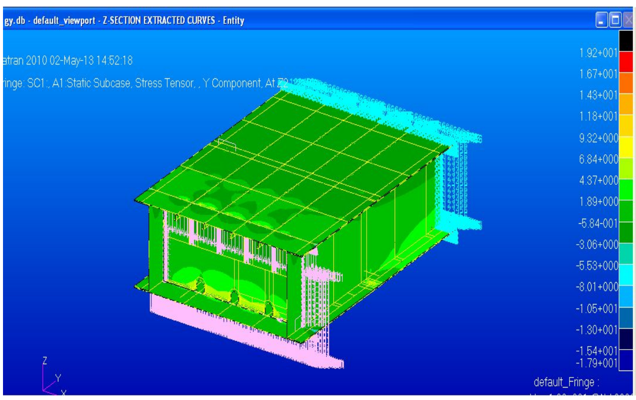

Figure 7 Results of Global analysis

Figure 8 Location of Maximum stress

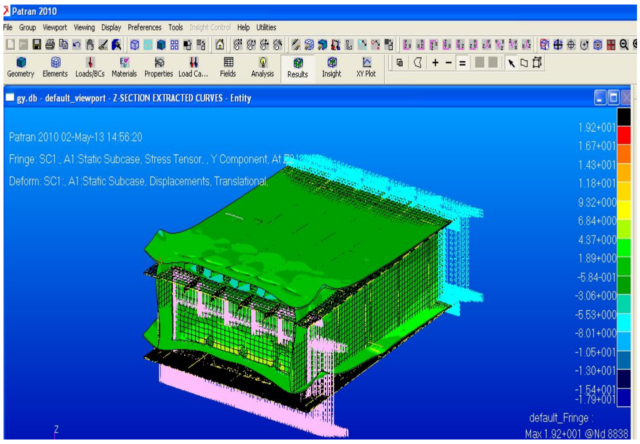

Figure 9 Deflection of the wing box

The stress distribution for the applied loads were observed and that exposes the stress is distributed uniformly but maximum stresses are developed nearer to spliced joint exactly at the rivets which connects spar and bottom skin as shown in Figure 11. The magnitude of stress developed here is 19.4kgmm^{-2}. Since the maximum stress we getting is at the same location we do local analysis on the specific location. It includes skin spliced region which we can take as bottom skin and the lower stringer region. Max Stress at Beam element 87995 near the splice joint so local analysis has to be carrying out for that region. The exact location of maximum stress from global analysis is created in PATRAN for local analysis with the help of geometrical tools. It is then meshed separately forming different groups. Final solid modeling including corresponding parts for local analysis has been shown in Figure 11.

The structure is safe because the stress magnitude which was obtained from the analysis is less than the yield strength of the structural material. Once wing box is safe from linear static analysis, next step is the fatigue life prediction of the wing box

4.2. Local Analysis Results

As in the case of global analysis, the particular area considered for local analysis undergoes tension in bottom skin. In order to create the same surrounding, we constrain any one or two translation direction, hence we took two cases.

Case 1: With z translation constraint

Case 2: With x and z translation constraint

During different iteration the maximum stress is found out to be 25.3kgmm^{-2} and 25.5kgmm^{-2}

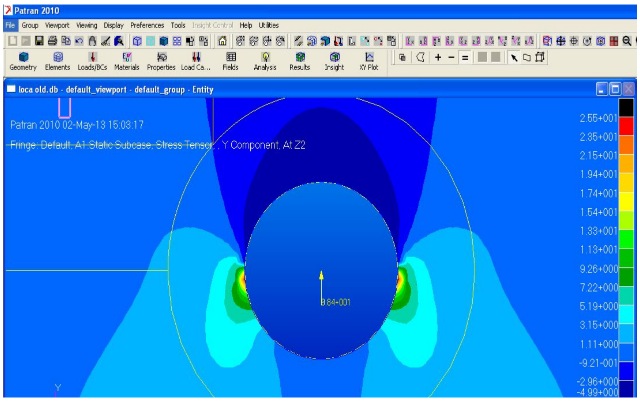

Figure 10 Local analysis result without fine meshing

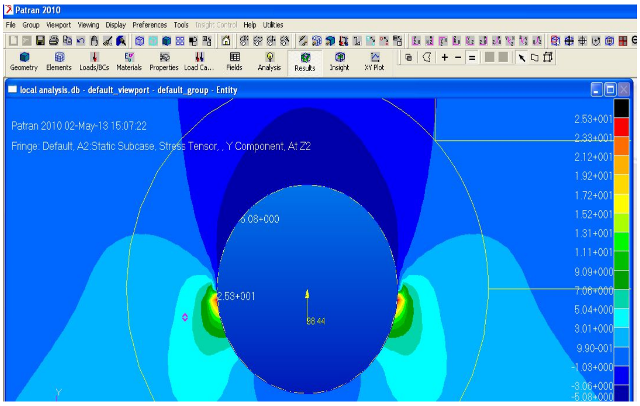

Figure 11 Local analysis with fine mesh

4.3. Iterations

Five iterations were carried out in the local analysis by changing the size of the element around the hole. By reducing the mesh of the element from coarse to fine, we can obtained the more accurate stress value at the rivet hole. The element size and mesh values are mentioned in the following figures.

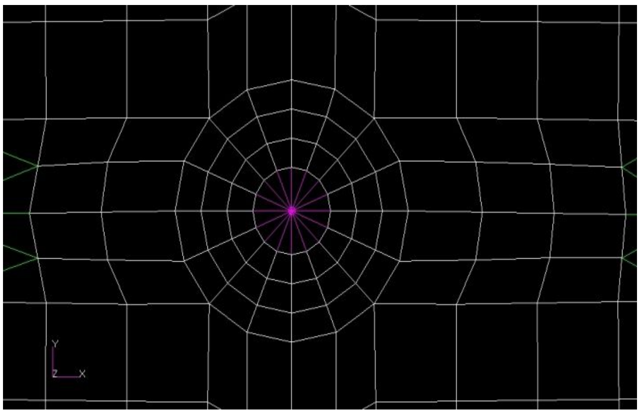

Figure 12 Elem Size 0.97mm

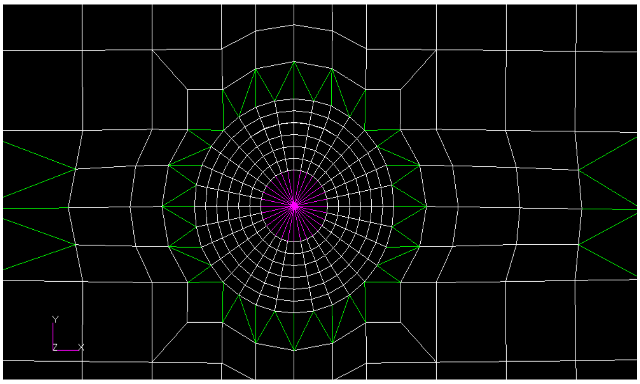

Figure 13 Elem Size0.49mm

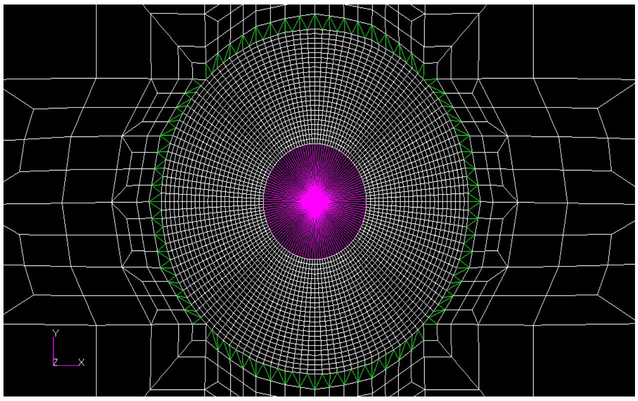

Figure 14 Elem Size 0.122mm

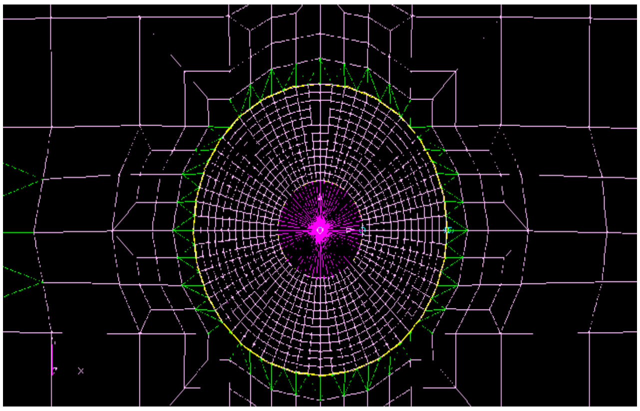

Figure 15 Elem Size 0.32mm

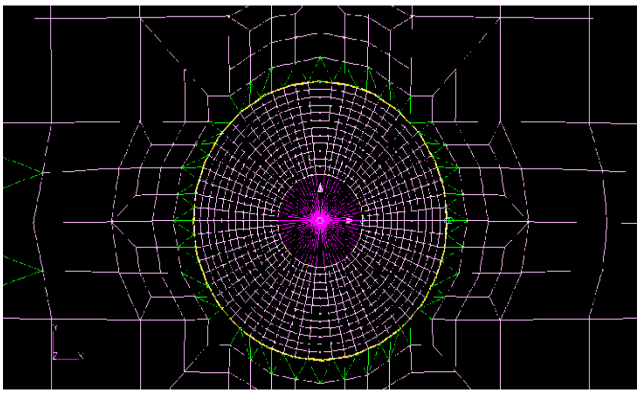

Figure 16 Elem Size 0.24mm

4.4. Summary of Results for Iteration

Table 3 Element edge Vs tensile strength

Element edge length (mm)	Max.tensile strength ($kgmm^{-2}$)
0.97	21.4
0.49	24.2
0.32	24.5
0.24	25.1
0.12	25.3

5. THEORETICAL CALCULATION

The stress values which are obtaining from finite element analysis are justified by strength of materials method.

By considering the section A-A

Bending moment at A-A $=p*x$ (1)

Due to this bending moment top skin undergoes compression and bottom skin undergoes tension. Thus

$=P * x = f_{\text{topskin/bottomskin}} * d$ (2)

From the above equation

$f_{\text{topskin/bottomskin}} = {p * x}/{d}$ (3)

$\sigma_{\text{topskin/bottomskin}} = \frac{f_{\text{topskin/bottomskin}}}{\text{cross sectional area}}$ (4)

Where

'p' is the distribution load applied on the wing box structure

'x' is the perpendicular distance between load and section

'd' is depth of the wing box ftopskin or bottomskin = force induced in the top skin or bottom skin

By considering the section 1087.5mm from the back end of the wing box the bending moment at the section A-A due to load is equal to 2610000kg-mm (5)

Bending moment at the section A-A based on tensile and compressive force induced in the top skin and bottom skin = ftop skin or bottom skin x d (6)

From the equations (5) and (6) load acting on the ftop skin or bottom skin = 6460.396 kg

Tensile stress or compressive stress developing in the bottom skin or top skin = 2.9365 kg/mm^2

6. FINITE ELEMENT ANALYSIS RESULTS

The FEM results show that the stress values which are calculated through software are given below, by taking average value of stress values at a distance of 1087.5mm from the applied load is 2.8 $kgmm^2$.

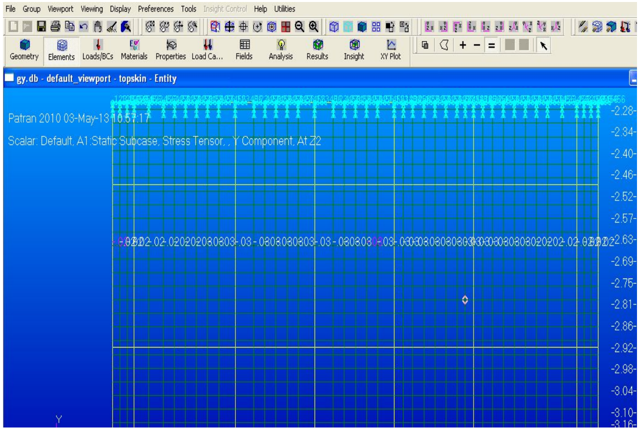

Figure 17 Stress values of top skin from software

We can able to calculate the local stress value in each and every element by marker option in the software. Thus the average stress value can be obtained by taking average of all local stress values of the elements.

7. CONCLUSION

Stress analysis of the wing box is carried out and maximum tensile stress is identified at one of the rivet holes near splice joints which is found out to be lower than yield strength of the material. Local analysis is conducted for the specific region for maximum principle stress. By local analysis it is validated that the maximum stress is at the same rivet hole during global analysis. Maximum tensile stress of 192 N/mm^{-2} is observed in the wing box. Several iterations are carried out to obtain a mesh independent value for the maximum stress. A fatigue crack normally initiates from the location maximum tensile stress in the structure. The fatigue calculation is carried out for an estimation of life to crack initiation. Since the damage accumulated is less than the critical damage the location in the wing box is safe from fatigue considerations. Through calculations it is found that crack will not be initiate at this location and structure is under safe.

REFERENCES

[1] Adarsh Adeppa, Patil M S and Girish K E (2012), “Stress Analysis and Fatigue Life Prediction for Splice Joint in an Aircraft Fuselage Through an FEM Approach”, International Journal of Engineering and Innovative Technology (IJEIT), Vol. 1,No. 4, pp. 142-144.

[2] Amarendra Atre (2006), “A Finite Element and Experimental Investigation on the Fatigue of Riveted Lap Joints in Aircraft Applications”, May, Dissertation, Georgia Institute of Technology.

[3] Bhaumik, M. Sujata(2008),Fatigue failure of aircraft components, journal of engineering failure analysis, Elsevier, Vol.15,No. 19,pp.675-694.

[4] Hong-Chul Lee , Jae-man Choi , Bokwon Lee , Tae-Gu Kim (2007) Failure analysis of stress corrosion cracking in aircraft bolts, Elsevier,vol 14,No 8,pp. 209-217.

[5] Jan Siegl , Ivan Nedbal (2009) Fatigue crack growth history in damage tolerance design of aircraft structures, international journal of fatigue, Elsevier, Vol 31,No 5, pp. 1062-1067.

[6] JaapSchijve (2004), Fatigue of Structures and Materials”, Kluwer Academic Publishers.

[7] Kosec, G. Kovacic (2002), Fatigue cracking of an aircraft wheel, journal of engineering failure analysis, Elsevier, Vol.9, No.6, pp.603-609.

[8] LucjanWitek (2006), Fatigue analysis of the wing-fuselage connector of an agricultural air craft, journal of engineering failure analysis, Elsevier, Vol 13, No.9, pp. 572-581.

[9] Marcin Ciesielski a, Jerzy Kaniowski (2009),Determination of fatigue crack growth rate from fractographic analysis of a specimen representing air craft, international journal of fatigue,Elsevier,Vol.31, No.7,pp.1102-1109.

[10] Min Liao (2010), Fatigue analysis for CF-18 component wing, journal of procedia engineering, Elsevier, Vol.2, No.9, pp.1673-1682.

[11] Molent (2005), An experimental evaluation of fatigue crack growth, Journal of engineering failure analysis, Elsevier, Vol.12, No.27, pp.99-128.

[12] Sridhar Chintapalli , Mostafa S.A. Elsayed (2010),The development a preliminary structural design optimization method of an aircraft wing box skin stringer panels, journal of aerospace science and technology, Elsevier,Vol 14,No,10,pp.188-198.

[13] Xiong Y and Bedair O K (1999),“Analytical and Finite Element Modeling of Riveted Lap Joints in Aircraft Structure”, The American Institute of Aeronautics and Astronautics (AIAA) Journal, Vol. 37,No. 1, pp. 93-99

[14] Basil Sunny and Richu Thomas. Stress Analysis of a Splice Joint in an Aircraft Fuselage with the Prediction of Fatigue Life to Crack Initiation. *International Journal of Design and Manufacturing Technology (IJDMT).*5(3), 2014, pp.142–147.